

Numerical study of the evolution of vortices in a linearly stratified fluid (*)(**)

M. BECKERS⁽¹⁾, R. VERZICCO⁽²⁾, H. J. H. CLERCX⁽¹⁾ and G. J. F. VAN HEIJST⁽¹⁾

⁽¹⁾ *J. M. Burgers Centre for Fluid Dynamics, Eindhoven University of Technology
Department of Physics - P. O. Box 513, 5600 MB Eindhoven, The Netherlands*

⁽²⁾ *Università di Roma "La Sapienza", Dipartimento di Meccanica e Aeronautica
via Eudossiana 18, 00184, Roma, Italy*

(ricevuto il 18 Novembre 1998; approvato il 6 Maggio 1999)

Summary. — This paper presents a numerical study in which the evolution of vortices in a stratified fluid is compared to the evolution of two-dimensional vortices. The influence of the Reynolds number and the Froude number are investigated, for the evolution of axisymmetric vortices, for their azimuthal instability and for the subsequent formation of tripoles. It is found that due to radial diffusion axisymmetric vortices with various initial vorticity profiles all evolve towards the same profile. This evolution reduces the growth of azimuthal instabilities which may lead to the formation of a tripole. For vortices in a stratified fluid the effect of the ambient stratification on the evolution of the vortices is investigated. It is found that a process of vortex stretching, which becomes more pronounced for increasing Froude numbers, leads to a weaker tripole formation.

PACS 92.10.Ei – Coriolis effects.

PACS 47.32.Cc – Vortex dynamics.

PACS 47.55.Hd – Stratified flows.

PACS 47.11 – Computational methods in fluid dynamics.

PACS 01.30.Cc – Conference proceedings.

1. – Introduction

Flows in a linearly density-stratified fluid show large resemblance with two-dimensional (2D) flows due to the presence of buoyancy forces, which strongly suppress vertical motions. Such 2D flows are characterized by the process of self-organization, *i.e.* small-scale turbulent structures evolve towards large-scale vortices (see, *e.g.*, [1]). Experiments on the evolution of turbulence in stratified fluids, in which the initial flow was forced by horizontal injection of a jet or by towing a rake through the fluid, have also revealed the formation of coherent vortex structures. In the first case dipolar

(*) Paper presented at the International Workshop on "Vortex Dynamics in Geophysical Flows", Castro Marina (LE), Italy, 22-26 June 1998.

(**) The authors of this paper have agreed to not receive the proofs for correction.

vortices were formed from the initially turbulent jet [2], whereas the rake forcing resulted in the formation of a large number of interacting pancake-like vortices [3]. In contrast to purely 2D turbulence these vortices are in fact three-dimensional (3D): although the vortical motion is planar, the finite vertical extent of the vortices implies vertical gradients in the flow. Recently a model was proposed that describes the vertical structure of axisymmetric pancake-like vortices [4]. This model shows that to a large extent the flow associated with vortices in a linearly stratified fluid can be considered as being quasi-2D. However, when the Froude number becomes larger, a 3D secondary circulation becomes increasingly important.

In a (non-rotating) stratified fluid vortex lines of pancake-like vortices should close within the fluid. This implies that a single monopolar vortex will be surrounded by a ring of opposite (vertical) vorticity. In purely 2D flows it was found that such shielded vortices can develop azimuthal instabilities when the steepness of the radial vorticity gradient exceeds a certain value [5]. This azimuthal instability can eventually lead to the formation of a tripolar vortex. Such a tripole formation was also observed in laboratory experiments in a stratified fluid [6]. In this paper it is investigated how the 3D character of the flow influences this tripole formation in comparison to the purely 2D case. Therefore, first the effects of viscosity on the evolution of purely 2D vortices are studied. Then the influence of the Froude number and Reynolds number on the azimuthal instability of pancake-like (3D) vortices is investigated.

2. – Numerical model

Numerical flow simulations have been performed, based on the time-dependent incompressible 3D Navier-Stokes equations and the equation describing the fluid's salinity, with the variables defined in a cylindrical coordinate system. The equations are written in the Boussinesq approximation, where a linear relationship between the salinity and the fluid density has been used, and all variables are scaled by appropriate constants. The density $\tilde{\rho}$ and the pressure \tilde{p} will represent deviations of the actual density and pressure from values in the ambient, linearly stratified fluid. The Navier-Stokes equations in the Boussinesq approximation are non-dimensionalized by introducing a velocity scale V , a length scale L , a pressure scale $\rho_0 V^2$ and a density scale defined by $(\rho_0/g) N^2 L$, where $N = \sqrt{-(g/\rho_0)(d\rho/dz)}$ represents the buoyancy frequency. The three dimensionless constants that result from the non-dimensionalization are the Reynolds number $Re = VL/\nu$, the Froude number $Fr = V/LN$ and the Schmidt number $Sc = \nu/\kappa$. The equations governing the fluid motion are given by

$$(1) \quad \frac{\partial \mathbf{v}}{\partial t} + \mathbf{v} \cdot \nabla \mathbf{v} = -\nabla p - \frac{1}{Fr^2} \tilde{\rho} \mathbf{e}_z + \frac{1}{Re} \nabla^2 \mathbf{v},$$

$$(2) \quad \nabla \cdot \mathbf{v} = 0,$$

$$(3) \quad \frac{\partial \tilde{\rho}}{\partial t} + \mathbf{v} \cdot \nabla \tilde{\rho} - v_z = \frac{1}{Sc Re} \nabla^2 \tilde{\rho}.$$

Details of the finite-difference method that is used to solve these equations in a cylindrical coordinate system, can be found in [7] and in [4]. The finite-difference algorithm is also suitable to simulate axisymmetric flows (*i.e.* simulations in the

(r, z)-plane only) and 2D flows (in the (r, θ) -plane). In the latter case the calculation of the density field is not necessary.

3. – Evolution of vortices in 2D flows

In 2D axisymmetric flows the vorticity equation is given by

$$(4) \quad \frac{\partial \omega}{\partial t} = \frac{1}{\text{Re}} \frac{1}{r} \frac{\partial}{\partial r} \left(r \frac{\partial \omega}{\partial r} \right),$$

where ω is defined as $\omega = (1/r)(\partial/\partial r)(rv_\theta)$. The equation, which has been non-dimensionalized like in the previous section, indicates that the vorticity evolution is

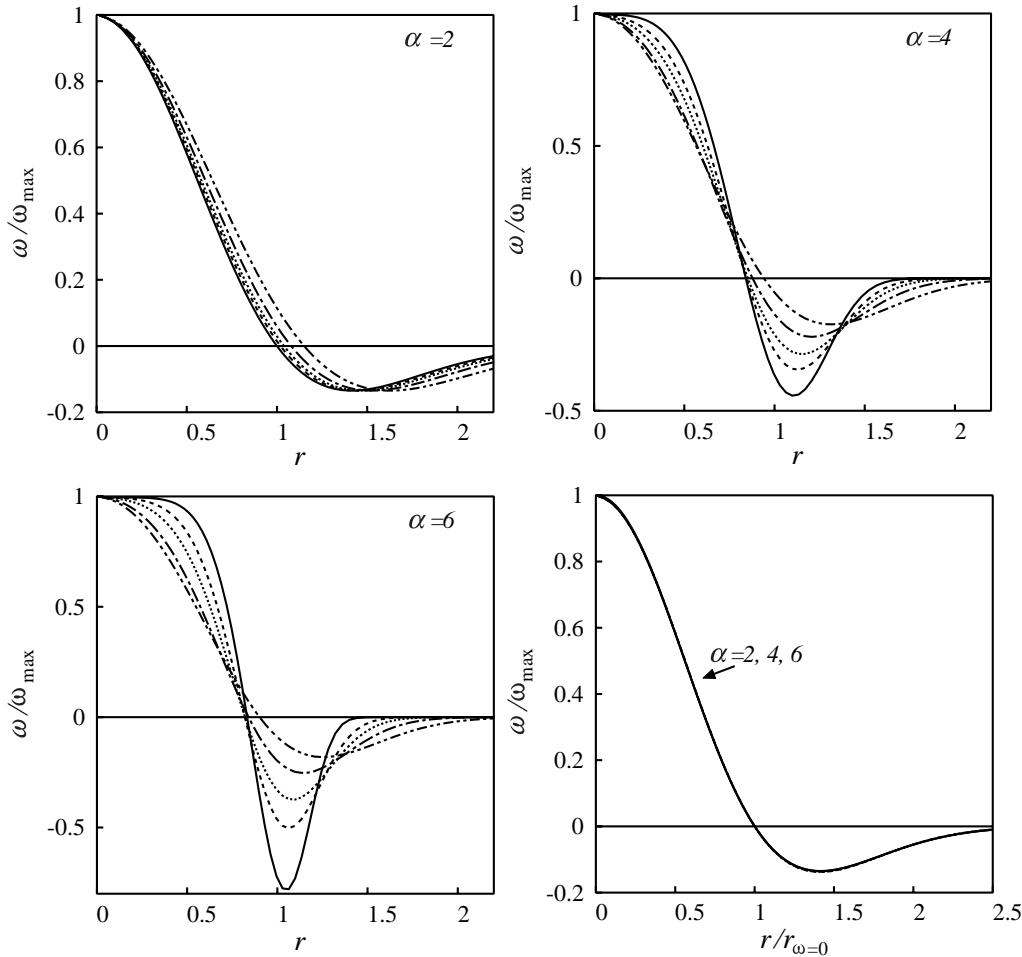


Fig. 1. – Temporal evolutions of 2D axisymmetric vortices with (a) $\alpha = 2$, (b) $\alpha = 4$ and (c) $\alpha = 6$, showing radial cross-sections of ω scaled by their maximum values, at $t/\text{Re} = 0, 0.01, 0.02, 0.04$ and 0.08 (with the continuous line for $t = 0$). (d) Comparison of $\omega(r)$ at $t/\text{Re} = 0.40$ for all three cases.

entirely governed by radial diffusion. The equation is solved for a shielded vortex with an initial vorticity distribution given by

$$(5) \quad \omega(r; \alpha) = \left(1 - \frac{1}{2} \alpha r^\alpha\right) \exp[-r^\alpha],$$

where α is called the steepness parameter (see [5]). It can be derived that for $\alpha = 2$ a self-similar solution describes the evolution of the vorticity in time [4]:

$$(6) \quad \omega(r, t) = \frac{1}{(1 + (4/\text{Re}) t)^2} \left(1 - \frac{r^2}{1 + (4/\text{Re}) t}\right) \exp\left[-\frac{r^2}{1 + (4/\text{Re}) t}\right].$$

For values of $\alpha \neq 2$ the solution of (4) is less trivial and numerical simulations were performed in order to investigate how the evolution deviates from the self-similar solution (6). The evolution of the initial vorticity profile (5) is shown in figs. 1a-c for $\alpha = 2, 4$ and 6 , respectively. Each figure displays the scaled vorticity as a function of r at various times. The evolutions for $\alpha = 4$ and 6 show that radial diffusion apparently leads to similar vorticity profiles at later times. This is illustrated in figure 1d, where radial profiles of ω are shown, with the radial coordinate scaled by its value for which $\omega = 0$. Remarkably the three initially very different vorticity profiles all collapse onto one single curve: profile (5) with $\alpha = 2$. To characterize this evolution of the vorticity profiles the variable $\gamma = |\omega_{\min}/\omega_{\max}|$ is introduced, which is the ratio between the extreme negative and positive vorticity values. For the self-similar decay of (6) its value is constant: $\gamma_2 = e^{-2} \approx 0.135$. For $\alpha = 2, 4, 6$ and 8 the evolution of γ is shown in fig. 2a. Note that these evolutions are independent of the Reynolds number, because in the diffusion equation (4) the time can be redefined as t/Re . For different initial values of α , the ratio γ eventually reaches the value γ_2 . During the diffusion process the vorticity profiles in figs. 1b and 1c were least-squares-fitted by the profile (5), which appeared to be a good representation at all times, and a value for α as a function of time was

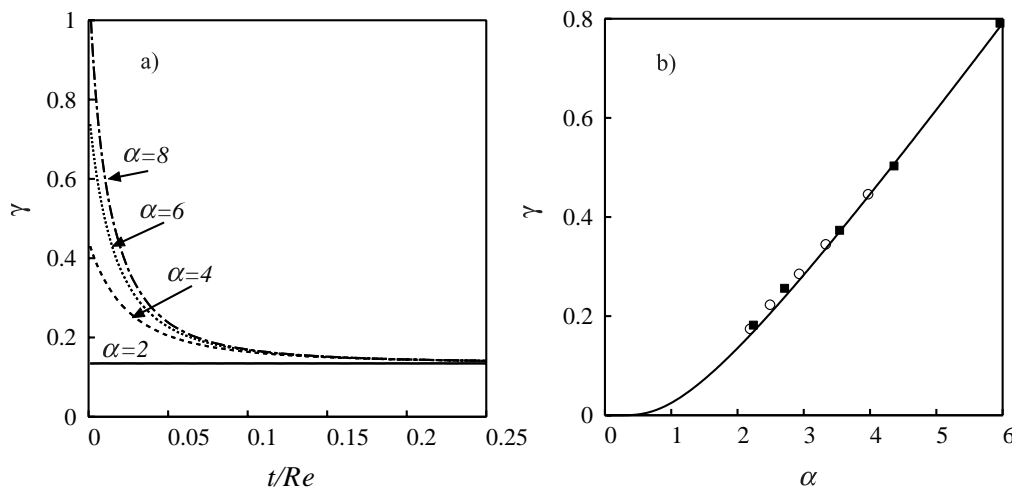


Fig. 2. – (a) Temporal evolution of the vorticity ratio γ for $\alpha = 2, 4, 6$ and 8 . (b) Relationship between the values of γ and α for the profile (5) and for the vorticity profiles in figs. 1b (circles) and 1c (squares).

determined. The relationship between the vorticity ratio γ and the steepness α of profile (5) is given in fig. 2b and for $t/Re = 0, 0.01, 0.02, 0.04$ and 0.08 the fitted value of α and the measured value of γ are shown. The combination of figs. 2a and b indicates that radial diffusion causes a decrease of the steepness of the vorticity profile of an axisymmetric vortex.

A linear stability analysis [8] for 2D vortices with a vorticity profile given by (5) revealed how the growth rate of various azimuthal wave numbers depends on the value of the steepness parameter α . For $\alpha < 1.85$ there is no growing unstable azimuthal mode, for $1.85 < \alpha < 3.0$ the mode-2 (*i.e.* the onset of a tripole) is the only unstable mode, and higher modes start to become unstable for higher values of α . Consequently, the decrease of γ during the viscous decay of the vortices will have implications for the development of azimuthal instabilities on initially axisymmetric vortices with $\alpha > 2$. The effect of viscosity on the formation of a tripole will be illustrated for a vortex with initially $\alpha = 4$. The instability of these vortices has been studied extensively for 2D flows, see, *e.g.*, [5,9,10], but only for (almost) inviscid conditions or for fairly high Reynolds numbers. In order to promote the possible instability, a small (1%) mode-2 azimuthal perturbation was added to the velocity field. In an inviscid 2D flow it was found [10] that for values of $\alpha > 3.2$ such a perturbation will initially result in the formation of a tripole; however, due to the effects of strain the core vortex breaks up and two separate dipoles are formed when each of the core vortices pairs with one of the satellites. Figure 3 shows the evolution of the vortex for two different Reynolds numbers, $Re = 1000$ and $Re = 3000$, respectively. For $Re = 3000$ indeed a breakup of

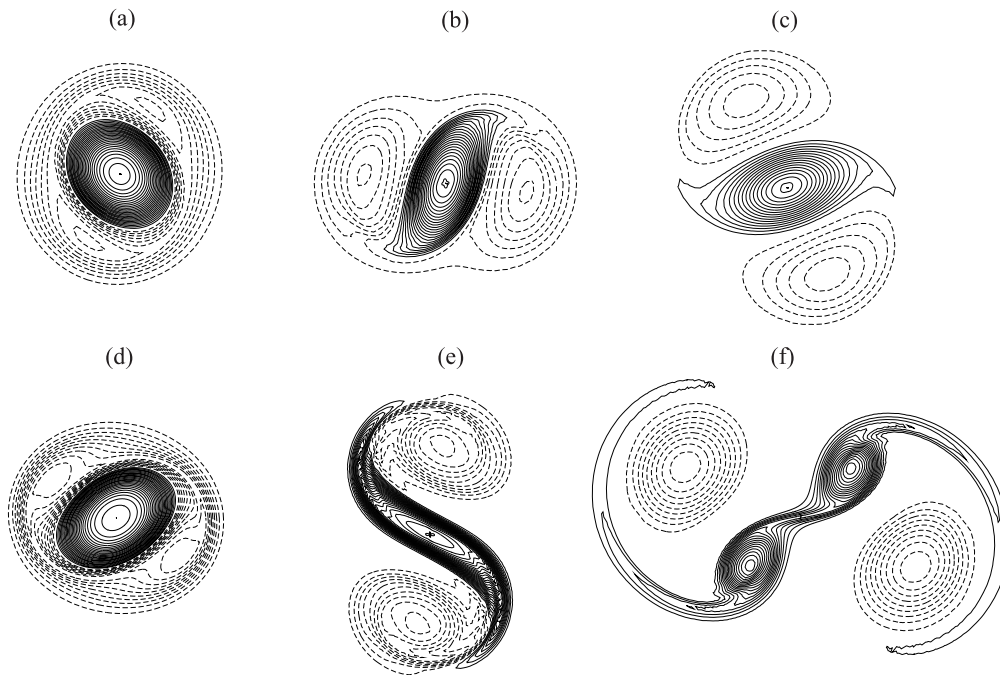


Fig. 3. – Contour plots of ω for the 2D evolution of an initially axisymmetric vortex with $\alpha = 4$ for $Re = 1000$ (a, b, c) and $Re = 3000$ (d, e, f). The evolution is shown for $t = 20$ (a, d) $t = 40$ (b, e) and $t = 80$ (c, f).

the core vortex takes place after an initial tripole formation, but for $\text{Re} = 1000$ only a tripole is formed. For even smaller Reynolds numbers the initial growth of the mode-2 perturbation is halted and no mature tripole is formed at all.

4. – The pancake vortex model

In this section a model is presented that describes the velocity and density distribution of a pancake-like vortex in a linearly stratified fluid, see [4]. The flow associated with such a vortex can be described in a first-order approximation as quasi-2D. This means that the flow is assumed to have only nonzero velocity components in the plane perpendicular to the density gradient, but this horizontal flow may still experience vertical shear. In order to describe the flow of initially axisymmetric vortices, a cylindrical coordinate system (r, θ, z) is defined with velocity components (v_r, v_θ, v_z) and with gravity acting in the negative z -direction. By using the incompressibility condition $\nabla \cdot \mathbf{v} = 0$ it can be found that for an axisymmetric flow ($\partial/\partial\theta = 0$) with no vertical motion ($v_z = 0$) also $v_r = 0$, so that $v_\theta(r, z, t)$ is the only nonzero velocity component. The Navier-Stokes equations (in the Boussinesq approximation and nondimensionalized) (1) then take the following form:

$$(7) \quad \frac{v_\theta^2}{r} = \frac{\partial p}{\partial r},$$

$$(8) \quad \frac{\partial v_\theta}{t} = \frac{1}{\text{Re}} \left(\frac{\partial^2 v_\theta}{\partial r^2} + \frac{1}{r} \frac{\partial v_\theta}{\partial r} - \frac{v_\theta}{r^2} + \frac{\partial^2 v_\theta}{\partial z^2} \right),$$

$$(9) \quad 0 = \frac{\partial p}{\partial z} + \frac{\tilde{q}}{\text{Fr}^2}.$$

where the Reynolds and Froude numbers are defined as before. Equation (8) shows that under the present conditions, *i.e.* with $\mathbf{v} = (0, v_\theta, 0)$ and $\partial/\partial\theta = 0$, the evolution of the velocity field is entirely governed by diffusion and eqs. (7) and (9) describe the cyclostrophic and hydrostatic balance of the flow, respectively. Combination of these two equations results, by eliminating the pressure, in a relationship between the azimuthal velocity field and the density distribution:

$$(10) \quad \frac{2v_\theta}{r} \frac{\partial v_\theta}{\partial z} + \frac{1}{\text{Fr}^2} \frac{\tilde{q}}{r} = 0.$$

This expression indicates that a vertical shear in the flow under the present conditions is only possible when there is a nonzero radial density gradient. In other words, according to this model, isopycnals will be deflected from their horizontal equilibrium shape in order to keep the flow in both cyclostrophic and hydrostatic balance.

Thus for a given velocity distribution $v_\theta(r, z)$ one can derive an expression for the perturbation of the density distribution $\tilde{q}(r, z)$. In [4] an (initial) velocity distribution was used, consisting of a radial part, corresponding to the vorticity distribution given by (5) and a vertical Gaussian distribution,

$$(11) \quad v_\theta(r, z) = \frac{1}{\sqrt{8\pi}} \frac{r}{\Lambda} \exp \left[-\frac{z^2}{2\Lambda^2} \right] \exp[-r^\alpha],$$

where Λ represents a measure of the initial vertical thickness of the vortex.

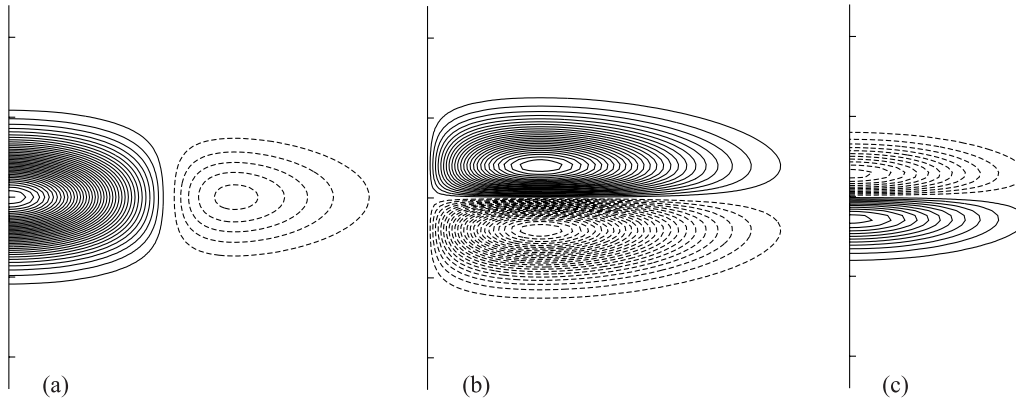


Fig. 4. – Spatial distributions in the (r, z) -plane of (a) $\omega_z(r, z)$, (b) $\omega_r(r, z)$ and (c) $\tilde{q}(r, z)$ according to the pancake vortex model. The dashed contours indicate negative values, while continuous contours denote positive values.

By substitution of (11) into (10) one derives

$$(12) \quad \frac{\partial \tilde{q}(r, z)}{\partial r} = \frac{2z \text{Fr}^2}{r\Lambda^2} v_\theta^2(r, z),$$

and by integrating the following expression for $\tilde{q}(r, z)$ is found:

$$(13) \quad \tilde{q}(r, z) = \frac{\text{Fr}^2 z}{4\pi\Lambda^4} \exp\left[-\frac{z^2}{\Lambda^2}\right] \int_r^\infty u \exp[-2u^\alpha] du.$$

From the velocity distribution (11), the distribution of the radial and vertical vorticity components can be determined by differentiation, according to their definitions. As an illustration for the case of $\alpha = 2$ the spatial distributions of $\omega_z(r, z)$, $\omega_r(r, z)$ and the corresponding $\tilde{q}(r, z)$, as given by (13), are plotted in fig. 4. It is easily observed that the vortex has a core of positive vertical vorticity, surrounded by a ring of negative vorticity (fig. 4a). The graph of the radial vorticity component ω_r (fig. 4b) indicates how the vortex lines form closed loops. The distribution of the density perturbation \tilde{q} (fig. 4c) shows that the isopycnals in both the upper and the lower halves of the vortex are deflected towards the midplane.

Numerical simulations [4] of the evolution of a vortex with initial velocity and density distributions given by (11) and (13) have revealed that during the viscous decay of the vortex, isopycnals relaxed towards their undisturbed (*i.e.* horizontal) shape. It was also observed that this resulted in a stretching of the vortex tubes in the centre of the vortex. This process is shown schematically in fig. 5. Furthermore, it was found that the stretching effect becomes stronger with increasing Froude number.

5. – Evolution of pancake-like vortices

The evolution of pancake-like vortices in a linearly stratified fluid is in two aspects different from their purely 2D counterparts. Firstly, vorticity will diffuse also in the

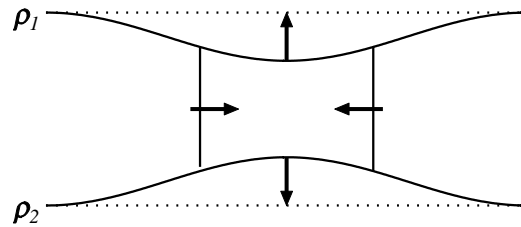


Fig. 5. – Illustration of the initial perturbation of two isopycnals (one above and the other below the vortex) and their relaxation to their undisturbed position. The arrows indicate the direction of the fluid motion and, consequently, the stretching of the vortex.

direction perpendicular to the plane of motion (*i.e.* vertical diffusion) and secondly vortex stretching, due to the perturbed isopycnals, will change the vorticity distribution. In this section a comparison is made between the evolution of a pancake-like vortex and a vortex in 2D flow. First the influence of the Froude number on the vorticity ratio γ is investigated for an axisymmetric vortex, then the formation of a 3D tripole is compared to its 2D counterpart. A more detailed study of the azimuthal instability of vortices in a linearly stratified fluid and of the 3D structure of tripoles is still in progress and results will be published elsewhere.

For two different values of α the decay of γ as a function of Re and Fr was investigated. The results are combined in fig. 6a and b, for $\alpha = 4$ and 8, respectively. The evolutions are given for $Re = 100$ and $Re = 1000$ and plotted in the same graph and time is again scaled by the Reynolds number. To ease comparison, the evolution of γ for the 2D flow is shown as well. It can easily be observed that γ decreases faster for flows with a larger Froude number, whereas for smaller Froude numbers (*e.g.*, $Fr = 0.1$) the decay of γ seems to coincide with the 2D situation. The enhanced decay of γ for increasing Froude number can be explained by the stretching process illustrated in fig. 5. This process causes a relative strengthening of the (positive) core, resulting in a stronger decrease of γ than induced by radial diffusion alone. Figure 6 also indicates that vertical diffusion does not influence the decay of the vorticity ratio, because for small Froude numbers stretching becomes negligible and the effect of vertical diffusion alone can be investigated. However, no appreciable difference with 2D flow can be found. Finally, the decay of γ of these 3D vortices appears to be weakly dependent on the Reynolds number (as can only be seen for $Fr = 0.8$), in contrast to real 2D flows, which are independent of Re (see fig. 2a).

For 2D flows it was shown that diffusion leads to a decay of γ and consequently to a more stable vortex. The enhanced decay of γ for increasing Froude numbers may even amplify this effect for the case of a pancake-like vortex in a stratified fluid. This hypothesis is investigated by the fully 3D simulation of a vortex with an initial velocity distribution given by (11) (with an azimuthal mode-2 perturbation of 1%) and a density perturbation given by (13), for the case of $\alpha = 4$ and $Re = 1000$. The simulation shown in fig. 3 illustrates that for a 2D flow these parameters result in a tripole. Figures 7a-c and d-f show horizontal cross-sections of the vertical vorticity at the vortex' symmetry plane at three stages of the evolution for $Fr = 0.1$ and $Fr = 0.8$, respectively. In the case of $Fr = 0.1$ the growth of a mode-2 perturbation can be clearly observed and this mode is amplified at later times, until at $t = 80$ (fig. 7c) a tripole has formed. For $Fr = 0.8$ the presence of the mode-2 perturbation can still be observed at $t = 20$ (fig. 7d), but it

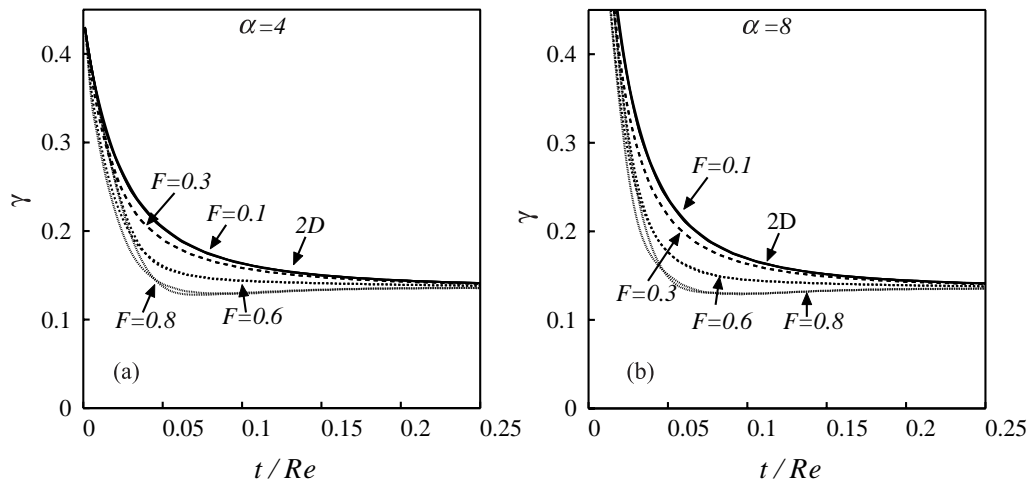


Fig. 6. – Temporal evolutions of γ for a 3D axisymmetric vortex with initially $\alpha = 4$ (a) and $\alpha = 8$ (b), for four different Froude numbers ($Fr = 0.1, 0.3, 0.6$ and 0.8). Results are shown for both $Re = 100$ and $Re = 1000$.

appears that this perturbation is not amplified as much as in the previous case. The tripole at $t = 80$ (fig. 7f) is therefore not so well developed; in comparison with the

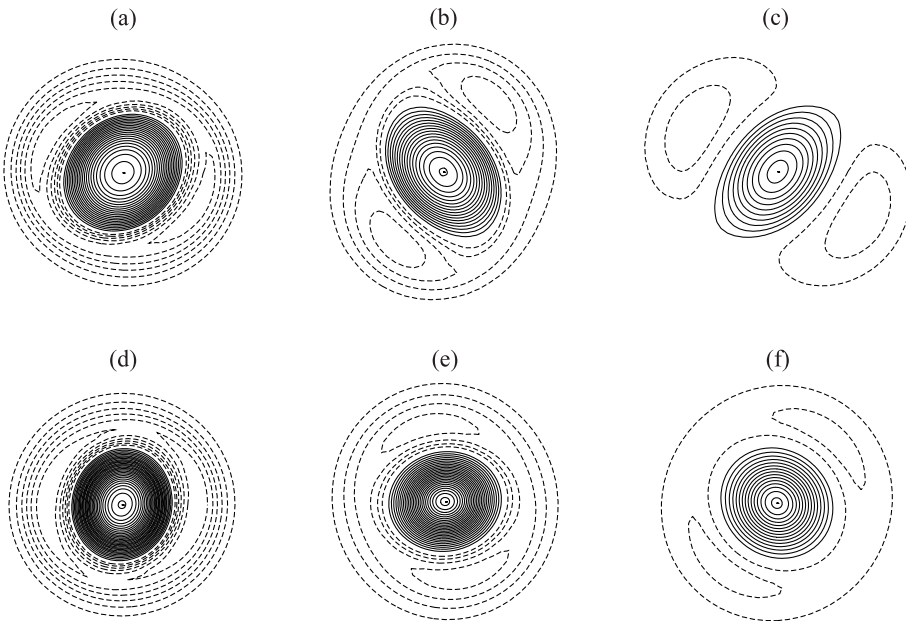


Fig. 7. – Contour plots of ω_z (at the vortex' symmetry plane) for the 3D evolution of an initially axisymmetric vortex with $\alpha = 4$ for $Re = 1000$ and $Fr = 0.1$ (a, b, c) and $Fr = 0.8$ (d, e, f). The evolution is shown for $t = 20$ (a, d) $t = 40$ (b, e) and $t = 80$ (c, f).

Fr = 0.1 case, the core is less elliptical and the negative vorticity is less concentrated in two satellites. Comparison with the 2D simulation shown in fig. 3a-c reveals that for small Froude numbers the evolution is similar, although vertical diffusion leads to a stronger overall decrease of the vorticity.

6. – Conclusions

In this paper the evolution of initially axisymmetric shielded pancake-like vortices in a linearly stratified fluid has been investigated and compared to that of their purely 2D counterparts. For the 2D case it was found that radial diffusion causes vorticity profiles with initially different shapes to evolve towards a single profile, which corresponds to a self-similar solution of the axisymmetric diffusion equation. The value of the ratio $\gamma = |\omega_{\min}/\omega_{\max}|$ of the vorticity profiles therefore decreases until a constant value is reached, which corresponds to the self-similar solution. It is shown that the value of γ of the various initial vorticity profiles is directly related to the steepness of the radial vorticity gradient, and this variable determines the growth rate of possible azimuthal instabilities. In particular, the decrease of γ by radial diffusion has the tendency to weaken the growth of the azimuthal instability that would lead to tripole formation. For a pancake-like vortex in a linearly stratified fluid (*i.e.* when 3D effects are present) the value of γ can also be affected by the stretching mechanism associated with the gradual reshaping of the isopycnals. During the viscous decay of the vortex isopycnals return to their equilibrium position and the fluid column between the isopycnals is stretched. This results in an enhanced decay of γ . As this stretching effect becomes more pronounced for larger Froude numbers, it was anticipated that the value of Fr influences the possible formation of a tripole. Fully 3D numerical simulations have confirmed this point of view. For Fr = 0.8 the formation of a tripole was observed to be much weaker than for the case of Fr = 0.1.

* * *

One of the authors (MB) gratefully acknowledges financial support from the Dutch Foundation of Fundamental Research on Matter (FOM).

REFERENCES

- [1] MCWILLIAMS J. C., *J. Fluid Mech.*, **146** (1984) 21-43.
- [2] FLÓR J. B. and VAN HEIJST G. J. F., *J. Fluid Mech.*, **279** (1994) 101-133.
- [3] FINCHAM A. M., MAXWORTHY T. and SPEDDING G. R., *Dyn. Atmos. Oceans*, **23** (1996) 155-169.
- [4] BECKERS M., VERZICCO R., CLERCX H. J. H. and VAN HEIJST G. J. F., submitted to *J. Fluid Mech.* (1999).
- [5] CARTON X. J., FLIERL G. R. and POLVANI L. M., *Europhys. Lett.*, **9** (1989) 339-344.
- [6] FLÓR J. B. and VAN HEIJST G. J. F., *J. Fluid Mech.*, **311** (1996) 257-287.
- [7] VERZICCO R. and ORLANDI P., *J. Comp. Phys.*, **123** (1996) 402-414.
- [8] CARNEVALE G. F. and KLOOSTERZIEL R. C., *J. Fluid Mech.*, **259** (1994) 305-331.
- [9] ORLANDI P. and VAN HEIJST G. J. F., *Fluid Dyn. Res.*, **9** (1992) 179-206.
- [10] CARTON X. J. and LEGRAS B., *J. Fluid Mech.*, **267** (1994) 53-82.